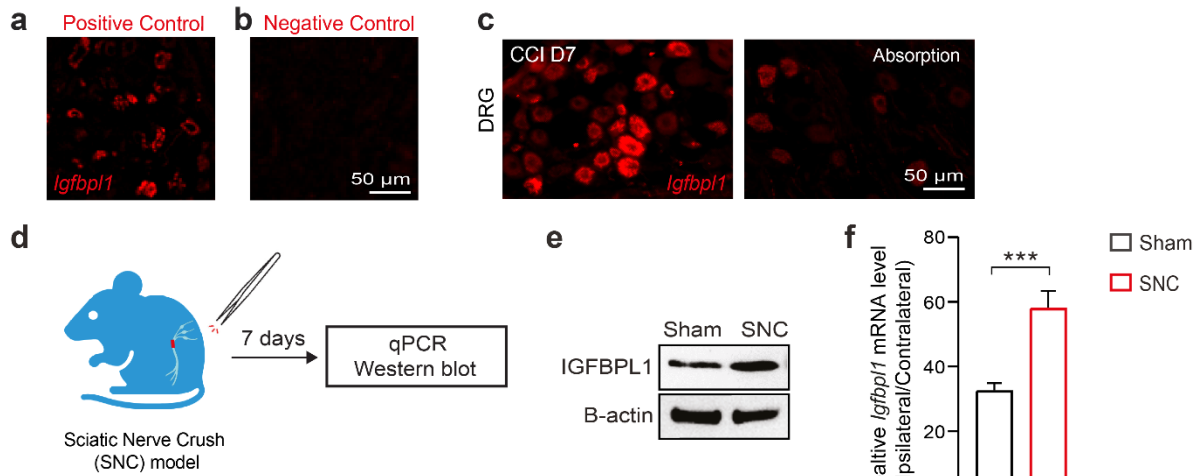


Supplementary Information

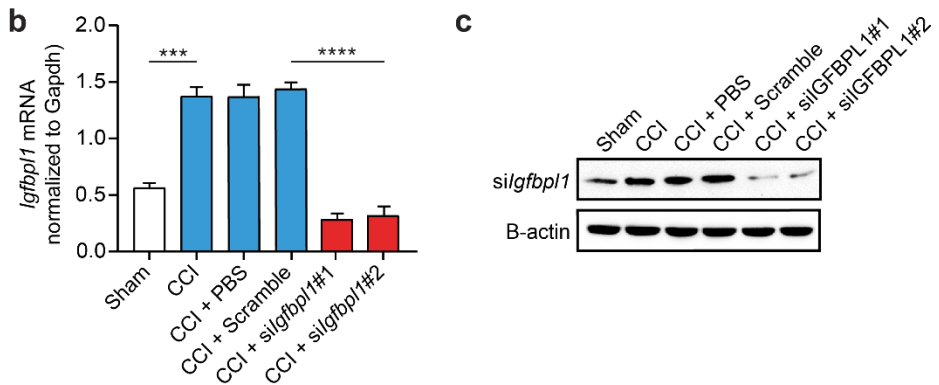
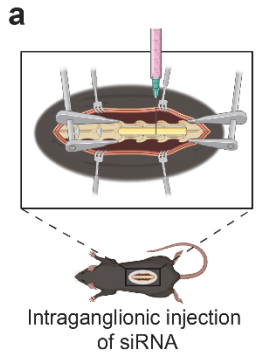
IGFBPL1 in DRG Nociceptors Drives Neuropathic Pain and Neuroimmune Crosstalk via IGF1R–ERK Signaling

Emmanuel Acquah¹, An Nazmus Sakib¹, Sang Seong Kim¹, Hyuk Sang Kwon¹,
Young Ro Kim^{2,3}, and Euiheon Chung^{1,4*}

*Corresponding author: Euiheon Chung, ogong50@gist.ac.kr

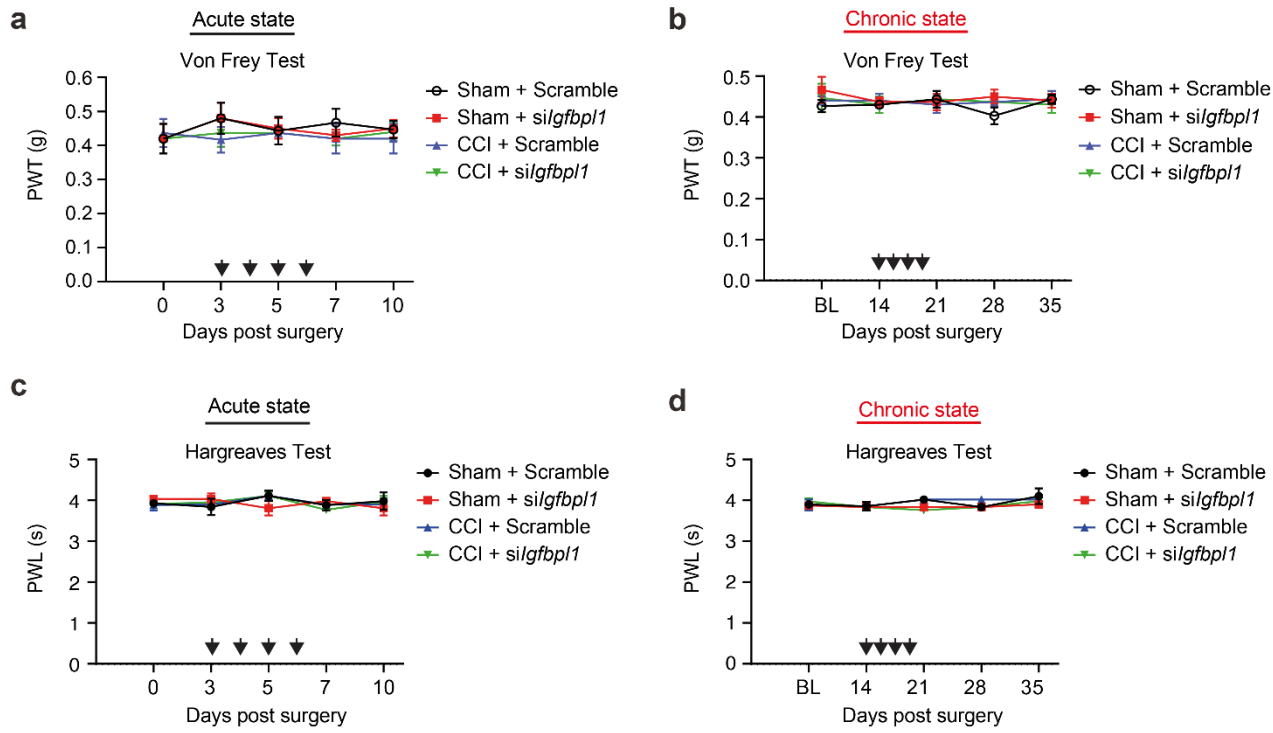


16
17
18 **Supplementary Fig. 1: The specificity of *Igfbp1* probe and antibody, and the**
19 **upregulation of *Igfbp1* mRNA and IGFBPL1 protein in Sciatic nerve crush (SNC).**
20
21
22
23
24
25
26
27
28 (a,b) RNAcope ISH of DRG sections of adult mice with the positive (a) and negative control (b). c The staining of DRG with *Igfbp1* antibody without (left) or with (right) absorption with *Igfbp1* peptide in Sham (c) or CCI mice (d) 7-day post-CCI surgery. $n=3$ mice per group. Scale bar, 50 μ m. d-f) Schematic representation of Sciatic Nerve Crush (SNC) model, where the sciatic nerve of the animal was subjected to crush injury. Tissue samples were collected on day 7 post-injury and analyzed by Western blot (d) and qPCR (e). A significant increase in *Igfbp1* mRNA and IGFBPL1 protein expressions were observed in the SNC compared to the Sham. β -actin used as a loading control. Data are presented as mean \pm SEM. *** $P < 0.001$. Student t test (F). $n=3$ mice per group.



Supplementary Fig. 2: *In vivo* knockdown of IGFBPL1 and validation.

(a–c) Experimental scheme (a) and validation of *siigfbp1* knockdown efficiency assessed by qRT-PCR (b) and western blot (c) after DRG-targeted injection. Student's t-test, $n = 4$ mice per group; *** $P < 0.001$, and **** $P < 0.0001$. All data are presented as mean \pm SEM.

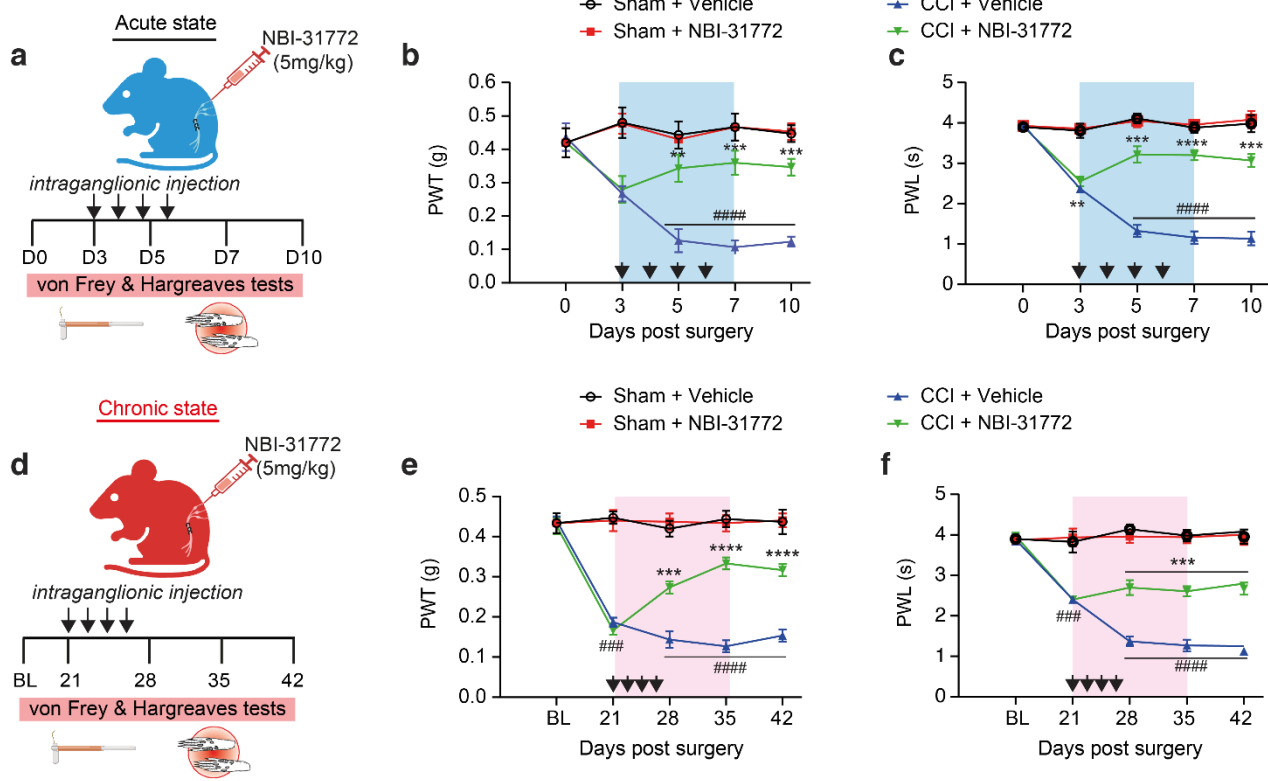


34
35

36 **Supplementary Fig. 3: Behavioral evaluation of mechanical and thermal pain**
37 **sensitivity in acute and chronic states following peripheral nerve Injury.**

38 **(a-d)** Behavioral tests evaluating paw withdrawal responses in acute and chronic states
39 using the Von Frey and Hargreaves tests across experimental groups: Sham + Scramble,
40 Sham + *siLFBPL1*, CCI + Scramble, and CCI + *siLFBPL1*. Acute state (Von Frey Test):
41 Intraganglionic injection of *siLFBPL1* in the contralateral DRG on post-CCI days 3 to 6
42 (acute phase) or days 14 to 17 (chronic phase) failed to attenuate CCI-induced mechanical
43 allodynia **(a,c)** and thermal hyperalgesia **(b,d)**. Two-way ANOVA followed by post hoc
44 Bonferroni's test, $n = 12$ mice per group. All data are presented as mean \pm SEM.

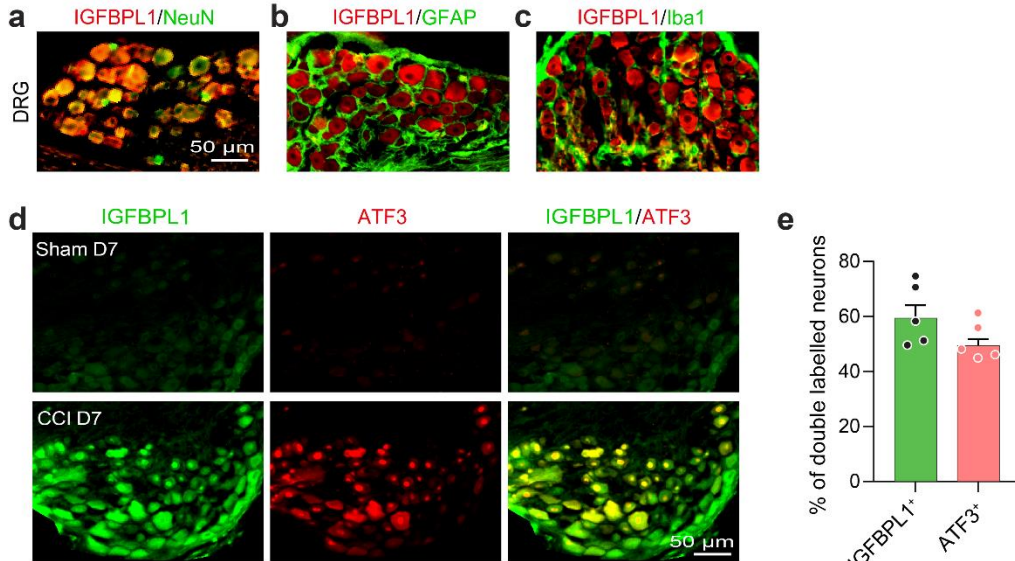
45



Supplementary Fig. 4: Pharmacological inhibition of IGFBP attenuated CCI-induced neuropathic pain.

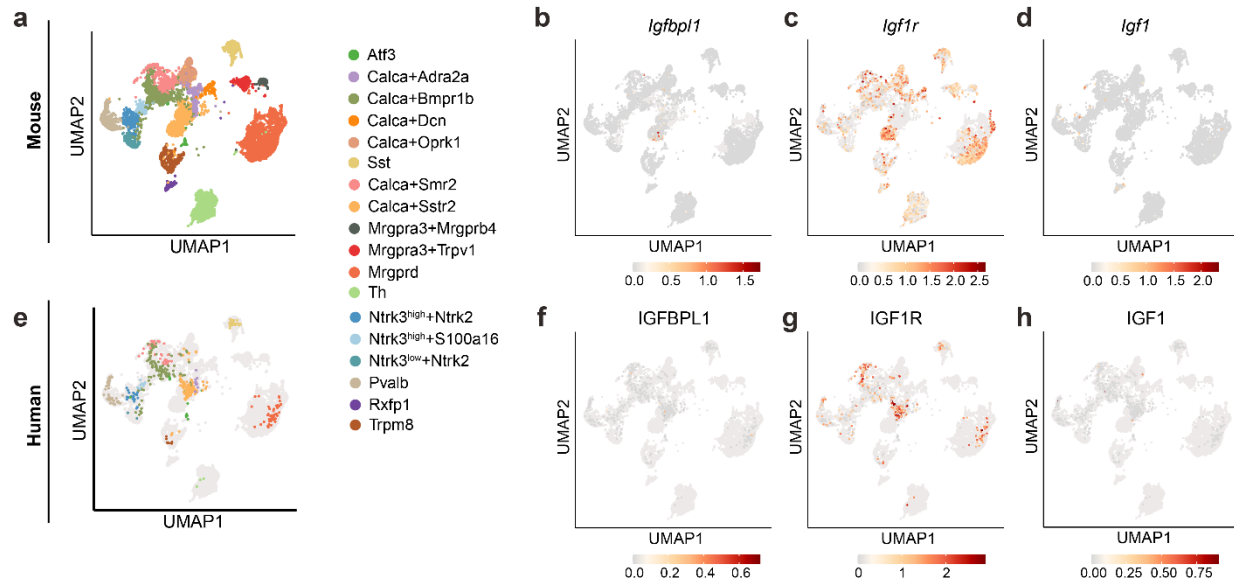
46
47

(a-d) Experimental scheme displaying timeline behavioral assessment after intraganglionic injection of NBI-31772 or vehicle in the ipsilateral DRG in Sham or CCI mice. **(b,c)** Mechanical **(b)** and thermal **(c)** hyperalgesia in mice after NBI-31772 injection during the acute phase. **(e,f)** Mechanical **(e)** and thermal **(f)** hyperalgesia in mice after NBI-31772 injection during the chronic phase. Two-way ANOVA followed by post hoc Bonferroni's test, $n = 12$ mice per group. * $P < 0.05$, ** $P < 0.01$, and *** $P < 0.001$; ##### $P < 0.01$ and ##### $P < 0.001$. All data are presented as mean \pm SEM.



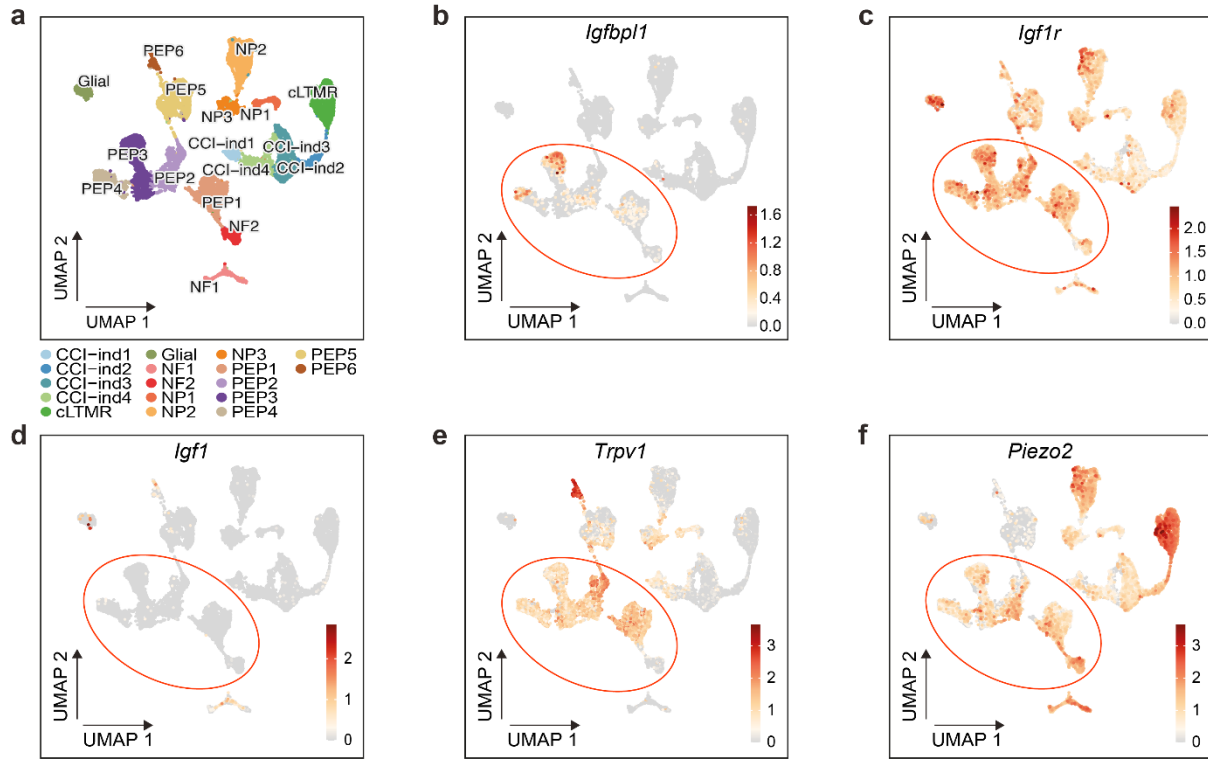
59 **Supplementary Fig. 5: The cell type distribution of IGFBPL1 and co-localization with**
 60 **ATF3 in the DRG.**

61 (a-d) Representative images of co-localization of IGFBPL1 with NeuN (a), GFAP (b) and
 62 Iba-1 (c) in mouse DRG. Scale bar, 50 μ m. f Double staining of IGFBPL1 and ATF3 in the
 63 DRG. Scale bar, 50 μ m. e Percentage of double-labeled neurons in IGFBPL1⁺ and ATF3⁺
 64 double-labeled neurons.



Supplementary Fig. 6: *Igfbpl1* expression in the mouse and human DRGs.

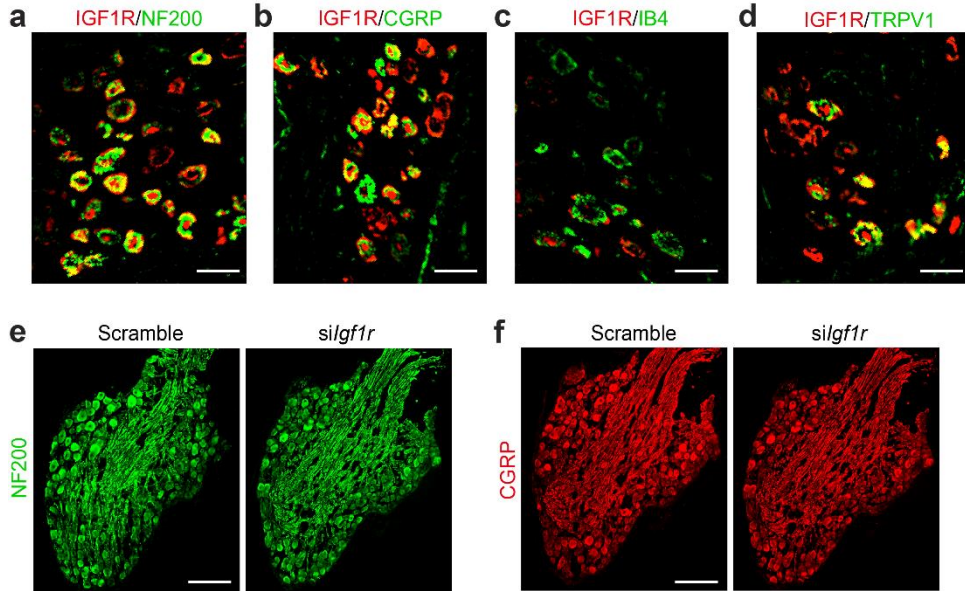
(a–h) UMAPs displaying clusters of DRG neuronal subtypes (a,e), injury-induced gene *Atf3* and the expression of IGF-related genes in mouse (*Igfbpl1*, *Igf1r* and *Igf1*) (b–d) and human (*IGFBPL1*, *IGF1R* and *IGF1*) (f–h) from scRNA-seq dataset⁴³.



Supplementary Fig. 7: *Igfbp1* expression in the mouse DRG neurons after CCI.

(a–f) UMAP displaying 17 clusters of DRG cell populations (neurons and glia cells), and the expression patterns of *Igfbp1*, *Igf1r*, *Igf1*, *Trpv1* and *Piezo2*. High *Igfbp1* expression is localized predominantly within specific neuronal subpopulations (indicated by red circle).

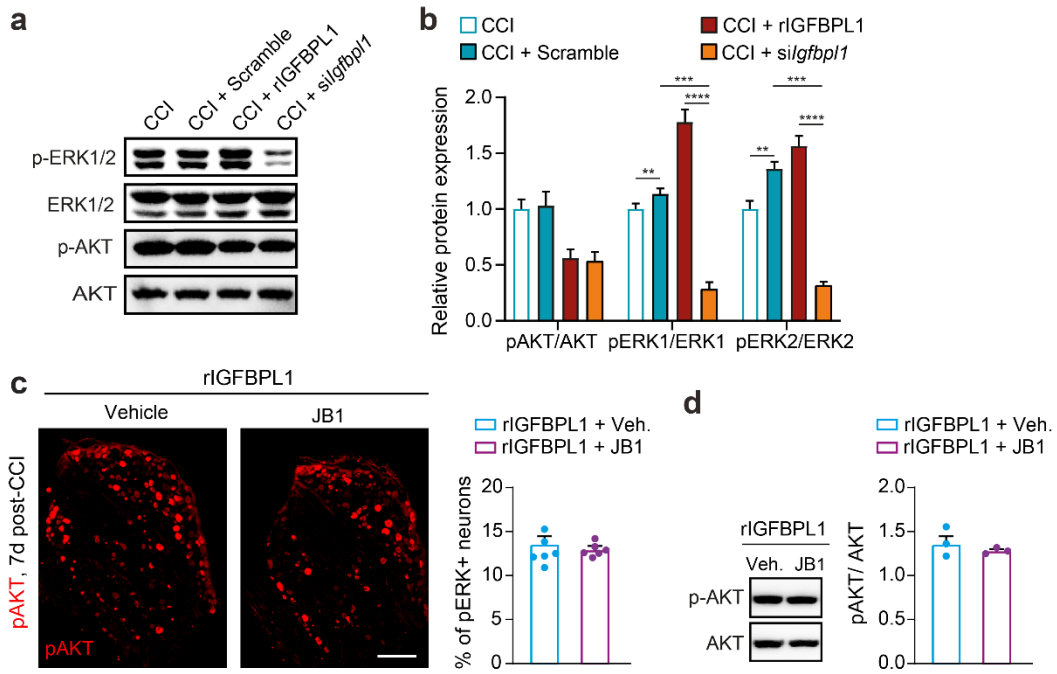
From scRNA-seq dataset⁴⁴.



78
79
80

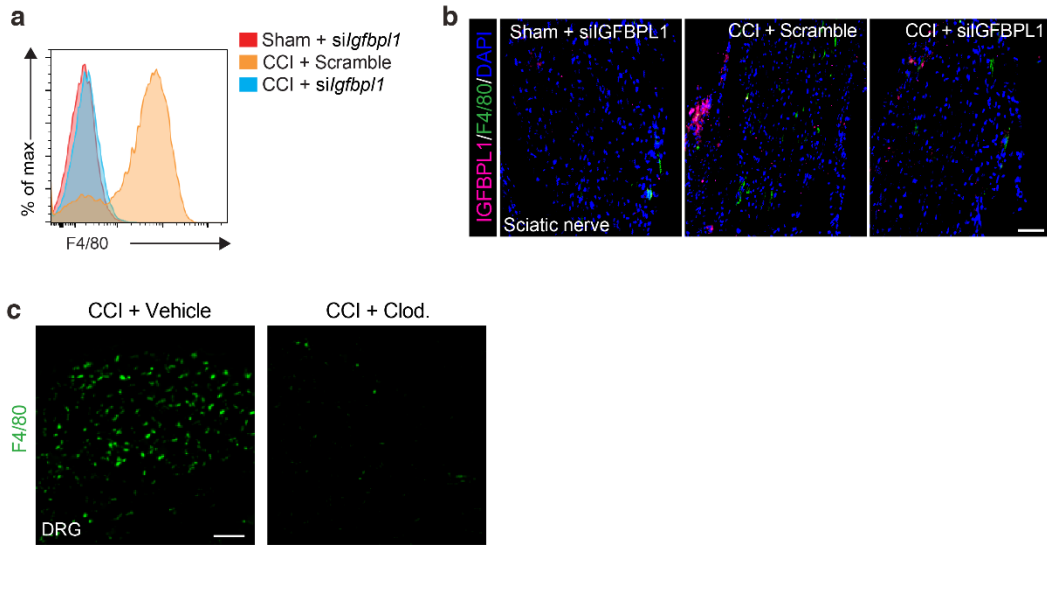
81 **Supplementary Fig. 8: Distribution of *Igf1r* mRNA in the DRG and the effects of**
82 **IGF1R knockdown.**

83 (a–g) Representative image of RNAcope showing the co-localization of *Igf1r* with NF200
84 (a), CGRP (b), IB4 (c) and TRPV1 (d) in the DRG. (e) Percentage of double-labeled
85 neurons in NF200⁺, CGRP⁺, IB4⁺ and TRPV1⁺ neurons. *Igf1r* knockdown mice show
86 normal distribution patterns of NF200 (e), and CGRP (f) in the DRG. Percentage of NF200⁺
87 and CGRP⁺ neurons. $n = 3$ mice/group. Scale bar, 50 μ m and 100 μ m.



Supplementary Fig. 9: The effect of pAKT pathway in IGFBL1 and IGF1R-mediated pain behaviors.

(a, b) Western blot analysis and quantifications showing pERK (a) and pAKT (b) expression in DRG neurons from mice with *Igfbpl1* knockdown or rIGFBPL1 overexpressed conditions. **(c, d)** Representative IHC staining and quantification of pAKT after intraganglionic JB-1 and rIGFBPL1 injection. $n=6$ mice. Scale bar, 100 μ m. **(d)** Immunoblotting analysis and quantification of pAKT protein expression in DRG neurons after JB-1 and rIGFBPL1 injection in CCI mice. $n=4$ mice per group. Two-way ANOVA followed by post hoc Bonferroni's test, $n=8$ mice per group. $*P < 0.05$, and $**P < 0.01$. All data are presented as mean \pm SEM.



Supplementary Fig. 10: The effects of IGFBPL1 inhibition and macrophage depletion on DRG macrophages.

a Flow cytometry analysis of F4/80⁺ cells isolated from DRGs following intraganglionic injection of *siIgfbp1* ($n = 3$ independent experiments). **b** Representative immunostaining images showing IGFBPL1⁺ cells (magenta), F4/80⁺ macrophages (green), and nuclei (DAPI, blue), with reduced infiltrating macrophages after *Igfbp1* knockdown ($n = 5$ mice per group; scale bar, 50 μ m). **c** Representative immunostaining images of F4/80⁺ cells in DRGs collected from vehicle or clodronate-treated mice after rIGFBPL1 injection. Chlodonate treatment reduced the number of macrophages (scale bar, 50 μ m).

Table S1. List of antibodies used in this study

Antibody	Species	Company	Cat. No.	RRID
anti-IGFBPL1	Goat	R&D	Cat# AF4130	AB_2279980
anti-IGF-1	Mouse	R&D	Cat# AF791	AB_2248752
anti-IGF1R	Mouse	R&D	Cat# MAB391	AB_2122409
anti-pIGF1R	Rabbit	SCB	Cat# sc-81499	AB_2797366
IgG	Rabbit	CST	Cat# 2729P	AB_1031062
anti-pERK1/2	Rabbit	CST	Cat# 4370	AB_2315112
anti-ERK1/2	Rabbit	CST	Cat# 4695	AB_390779
anti-pAKT	Rabbit	CST	Cat# 9271	AB_329828
anti-AKT	Rabbit	CST	Cat# 9272	AB_329827
NF200	Mouse	Millipore	Cat# MAB5266	AB_11212783
IB4-FITC	Mouse	Sigma	Cat#L2895	AB_477295
CGRP	Rabbit	CST	Cat#14959S	AB_2650536
TRPV1	Mouse	Abcam	Cat#ab203103	AB_443297
TRPV1	Rabbit	Alomone labs	Cat#ACC-030	AB_10008453
GS	Rabbit	ABclonal	Cat#A21822	AB_2735178
NeuN	Rabbit	Abcam	Cat#ab177487	AB_444290
NeuN	Mouse	CST	Cat#94403S	AB_2830192
GFAP	Mouse	CST	Cat#3670S	AB_2223032
IBA-1	Rabbit	ProteinTech	Cat#10904-1-AP	AB_2315043
TUBB3	Rabbit	Abcam	Cat#ab52623	AB_880896
ATF3	Rabbit	CST	Cat#18665S	AB_2723386
CD11b	Rat	BioLegend	101212 (APC)	AB_312784
F4/80	Rat	BioLegend	123110 (PE)	AB_893653
CD68	Rat	BioLegend	137012 (APC)	AB_893654

116

Table S2. The specific primers used for qRT-PCR in this study

Gene	Forward Sequence	Reverse Sequence
<i>Igfbp1_1</i>	ATGCCCCCTCGAGATATTCA	CTCGCACCTGGACAGCTATA
<i>Igfbp1_2</i>	GTGAGGGCTGTGCCTACCC	CATCACATGCGGTATCGGG
<i>Igf1r</i>	GTACCGGCACAACACTACTGCT	AGCCTGCTTCTCAGCTTCAG
<i>Tnf-α</i>	TGATCGGTCCCCAAAGGGAT	TGTCTTGAGATCCATGCCGT
<i>Il-6</i>	CAACGATGATGCACTTGCAGA	GTGACTCCAGCTTATCTCTGGT
<i>Il-1β</i>	TGCCACCTTTGACAGTGATG	AAGGTCCACGGAAAGACAC
<i>Ccr2</i>	ATCCACGGCATACTATCAACA	CAAGGCTACCATCATCGTAG
<i>Gapdh</i>	ATCACTGCCACCCAGAAGACT	ATGCCAGTGAGCTTCCCGTT

117

118

119

120

121

Table S3. The siRNA sequences used in this study

Target gene	Sequence sense (5' to 3')	Sequence antisense (5' to 3')
IGFBPL1_847	GCUCCCGAUGACCGCAUGUTT	ACAUGCGGUCAUCGGAGCTT
IGFBPL1_482	GCGAGUUUCGCUCCUGUGGUTT	ACCACAGGAGCGAACUCGCTT
Neg. Control	UUCUCCGAACGUGUCACGUTT	ACGUGACACGUCGGAGAATT

122